

Received 19 April 2024, accepted 12 May 2024, date of publication 17 May 2024, date of current version 24 May 2024.

Digital Object Identifier 10.1109/ACCESS.2024.3402264

RESEARCH ARTICLE

Prediction of Fault for Floating Photovoltaics via Mechanical Stress Evaluation of Wind Speed and Wave Height

BYEONG YONG LIM^{1,2}, SEONG-HYEON AHN^{1,2}, MIN SOO PARK³, JIN HO CHOI^{2,4}, HOONJOO CHOI^{1,2}, AND HYUNG-KEUN AHN^{1,2}, (Member, IEEE)

¹Department of Electrical Engineering, Konkuk University, Gwangjin-gu, Seoul 05029, South Korea

²Next Generation PV Module and Power System Research Center, Konkuk University, Seoul 05029, South Korea

³SK Hynix, Icheon-si, Gyeonggi-do 17336, South Korea

⁴Chungbuk Technopark Next Generation Energy Center, Jincheon-gun, Chungcheongbuk-do 27872, South Korea

Corresponding author: Hyung-Keun Ahn (hkahn@konkuk.ac.kr)

This work was supported in part by Human Resources Development Program of Korea Institute of Energy Technology Evaluation and Planning (KETEP) Grant funded by the Ministry of Trade, Industry and Energy, Republic of Korea, under Grant RS-2023-00237035.

ABSTRACT The escalating demand for environmentally sustainable energy sources in response to climate change necessitates the expansion of renewable power generation, particularly in the field of photovoltaic (PV) technology. Continuous advancements in PV power generation have substantially reduced production costs and chronic initial defects in PV modules. Effective PV power generation requires meticulous consideration of the installation structures and site selection processes. However, the identification of suitable power-generation locations often encounters challenges associated with civil complaints and environmental impediments. Floating Photovoltaic (FPV) systems positioned on water bodies have emerged as a promising solution for mitigating the environmental concerns associated with ground-based installations. This study endeavors to scrutinize the reliability of PV modules within water-based FPV systems by leveraging climate data for analysis. Module deformation is forecasted through material simulations, and the output values are estimated. An empirical pressurization experiment validates the actual alterations in the output values during a defect, thereby explaining the potential defect types. Considering the escalating investments in FPV power generation facilities, this study anticipates and assesses the potential defects and problems arising from natural disasters. The objective is to provide a robust predictive model for FPV power generation, encompassing dynamic simulations based on material properties and the outcomes of mechanical design of experiments on PV modules. The proposed methodology aims to provide scholarly insights into the judicious selection of FPV installation structures and optimal sites in placid water conditions and in circumstances characterized by strong winds and high oceanic waves. The proactive analytical framework enhances the decision-making processes concerning the installation and operation of FPV systems.

INDEX TERMS Floating PV, photovoltaic, PV simulation, PV degradation, PV fault detection.

I. INTRODUCTION

Climate change is driving the growth of renewable energy, including photovoltaic (PV) energy generation. PV is the most actively developed renewable energy sources, and the associated production costs are continuously decreasing

The associate editor coordinating the review of this manuscript and approving it for publication was Ton Duc Do¹.

owing to continuous technological developments [1], [2]. The inherent initial defects in the PV modules have also been greatly reduced. A PV power system requires the installation of a structure and selection of the corresponding area [3]. In the process of selecting a power generation site, many problems continue to occur because of complaints and environmental obstacles. To compensate for this, PV power generation infrastructure can be developed on water bodies,

which allows for more independent development from the crucial environmental problems that occur on land [4], [5].

The PV research is being conducted on both electrical and mechanical reliabilities, encompassing components such as PV panels, cables, and inverters. Particularly, issues related to system problems including overheating, malfunctions, and short circuits, as well as the stability of components, are actively being researched. Research is also being added on the stability of efficiency and power generation of PV to enable long-term stable power generation. With the increasing installation of floating PV systems, related research and data are gathered. FPV requires durability against environments such as seawater, wind, waves, and salinity compared to ground-mounted PVs. As FPV need to be installed on water, ensuring their location and structural stability is crucial. Research must explore various scenarios and forms of defects that may occur in maritime environments. Long term reliability assessments and technological developments tailored to maritime environments should be counted. This paper presents expectations regarding the durability of FPVs in marine environments. The defects were predicted based on climate data from specific locations in maritime environments. Based on experimental results, this paper demonstrates predictions of faults through simulation of FPV system under environmental conditions.

The FPV research have been conducted on the cost effectiveness of systems utilizing the geographical advantages. Compared to ground-mounted PV systems, FPV offers benefits such as higher efficiency, reduced water evaporation, and decreased CO₂ greenhouse gas emissions. As a result, FPV generation systems are being expanded in many countries. Due to positioning of the system on water, it offers advantages such as lowering module operating temperatures and increasing energy conversion efficiency compared to ground-mounted PV systems. Various simulations and theoretical studies have been conducted on this regard. FPV exhibits a high cooling effect due to water compared to ground PV. According to recent studies, FPV conversion efficiency has increased by 26.1%, resulting in an average generation yield increase of 5-6%. Particularly in arid and semiarid regions where water scarcity is a serious issue, using FPV modules to reduce water evaporation has been proposed through numerous studies. Research has shown that covering only 30% of the water surface with FPV systems can reduce evaporation by 49%, while 40% of water in open reservoirs is lost to evaporation. The number of FPV power plants is therefore, expected to increase continuously. Based on the advantages of FPV, this paper will examine factors related to the climatic conditions for FPV installation.

FPV systems offer advantages such as surface installation limitations and cooling effects [6]. Owing to their enormous potential, FPV systems can avoid conflicts with other industries and generate more power than ground-mounted PV system, thereby, playing a pivotal role in the generation and supply of clean energy [7]. In FPV systems, the reliability of PV modules, which is the most important factor, is analyzed using climate data and predicted by simulating the module

and deformation through the corresponding material simulation [8]. The actual change in the output value and type of defect were confirmed through an actual pressure test when the defect occurred [9].

This study proposes direct FPV power generation prediction through the pre-prediction of defects and problems caused by natural disasters owing to the increase in FPV power facilities and power generation [10]. Based on the results from the mechanical design of experiments (DOE) for each material property and PV module, a dynamic simulation conducted for the FPV module. The mechanical reliability of FPV modules will guide the selection of installation structures, and alternative for FPV installation and selection will be presented based on output prediction [11].

II. METHODS AND DATA ACQUISITION

The proposed method entails the following steps:

1. Collect climate data such as wind speed, wave height, and PV radiation.
2. Mechanical experiment and DOE using the collected climate data.
3. Simulate the deformation of PV modules for predicting fault detection.
4. Predict the output of PV modules using the analysis data.

Predictions are made regarding the location to be considered and the expected strength and reliability of the structures when installing them by analyzing the factors that can cause the deformation of objects in the natural environment. Forces related to natural environmental factors are summarized in Table 1, in which the impacts of wind speed, atmospheric pressure, and wave height on structures owing to direct wind forces were analyzed [12], [13].

Collecting climate data, such as temperature, water temperature, humidity, and pressure were measured 8 times a day, and the data were represented as averages of the data collected at regular intervals. In cases where measurements were not taken for any of the 8 measurements, the average of the data confirmed at 4 regular intervals was used. If data were measured less than once or up to 4 times, the missing data were replaced with the average of the data measured at the regular intervals excluding the unmeasured data. Additionally, for maximum/minimum values, the first observed value was initially adopted, and subsequently, the highest value among the data measured at regular intervals was substituted. When measurements were not taken at the time required for daily calculations or if values that did not meet the criteria for daily statistics were obtained, they were treated as "Data N/A." Wave data were calculated by analyzing 1024 spectra data sampled at 1-second intervals for water level measurements. Similarly, data for wind direction and wind speed were sampled using the same method and compared to process the maximum wind direction and speed.

The wind is generally generated by the movement of air, with temperature differences, pressure variances, and variations in terrain being primary causes. The temperature is a critical factor determining air density and warm air has

lower density than cold air. When there is a temperature gradient between different regions, air moves due to density differences, resulting in wind formation. The sea breezes between coasts and inland areas occur as warm air rises from the land to the sea during the day, while cold air flows from the sea to the land at night, leading to wind formation. The pressure differences in the air also contribute to the formation of wind, as air tends to move from high pressure areas to low pressure one, resulting in wind caused by these pressure differentials. Terrain influences wind formation, altering wind direction and intensity by modifying airflow paths. The wind speed is usually measured in meters per second (m/s) and is determined by wind velocity and the area of air. Air pressure is generated by the weight of air, influenced by air mass, gravity, and temperature. Air is attracted close to the surfaces both land and floating conditions due to gravity, resulting in higher pressure near the surface.

The pressure decreases with altitude as air becomes less dense. Although pressure varies across locations, average sea-level pressure is approximately 1013 hPa (1 millibar). The pressure changes significantly impact weather, with high pressure bringing clear skies and low pressure indicating cloudy and rainy conditions. on the floating surface.

The wave height denotes the height of waves generated in the ocean and is mainly determined by factors such as wave size, coastal shape, coastal topography, seabed features, wind speed, wind direction, and wave size. It is typically defined as the vertical distance between the crest and trough of a wave measured from the water surface. The wave height is a measure of the height waves rise above the mean wave level and is affected by factors such as wind strength, duration, seabed topography, tides, currents, and seismic activity. Stronger winds, deeper waters, and shoals can result in higher wave heights. To convert wave height into force, one needs to know its height and period, which exert direct pressure on floating bodies equipped with FPV modules. The wave height is the distance between the wave’s crest and trough.

TABLE 1. Environmental observation data to force.

Environmental Data	Observation Data		Force [N]	
	Avg.	Max.	Avg.	Max.
Wind Speed [m/s]	5.3	21.8	18	297
Atmospheric Pressure [hPa]	1,017.0	1,039.4	10	10
Wave Height [m]	2.32	10.1	5,826	25,364
Relative Humidity [%]	76.7	96.0	N/A	N/A
Temperature [°C]	13.4	28.2	N/A	N/A

An analysis of maritime conditions for the installation of offshore PV modules was conducted, utilizing observational data from a weather station in Buan, South Korea. The data, collected from 2020 to 2022, was used to analyze factors that may influence marine structures in the environment.

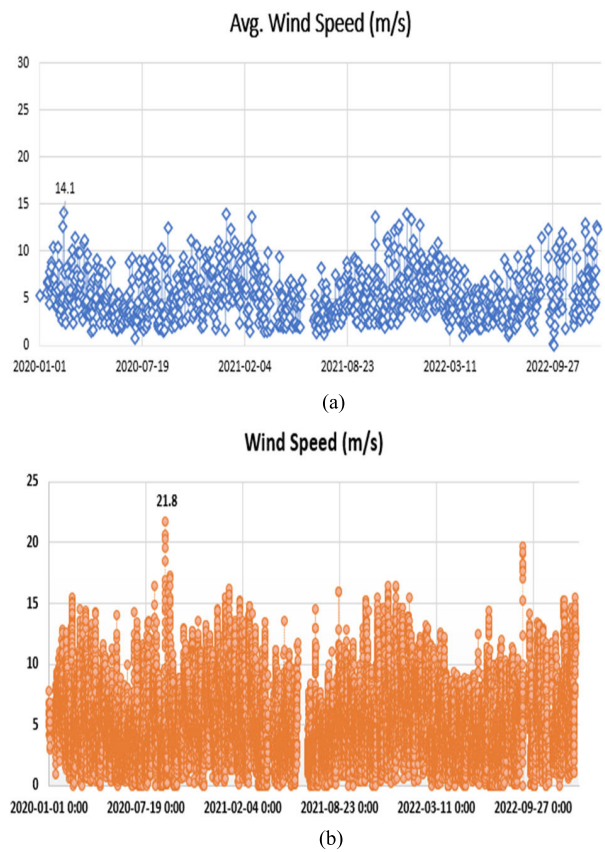


FIGURE 1. Wind speed at Buan, Korea: (a) daily averaged; (b) instantaneous.

Buan is located near the Saemangeum area and is a suitable location for planning a large-scale PV power plant, making it convenient for the analysis of offshore PV energy and enabling predictions based on the results in this location in the future [14].

The ocean environment data was measured using the observation equipment, Discus 3M buoy. The buoy used in this paper was installed at latitude N 35° 39' 09", longitude E 126° 11' 39", and measurements were taken for nine elements including temperature, wave height, wave period, wave direction, and water level. The offshore buoy was installed in a buoyant area at a depth of 25m, with the wave sensor at a depth of ~0.1m, temperature/humidity sensor at 3m, barometer at 0.2m, and wind direction/speed sensor at 3m for data measurement. The daily weather data were measured eight times, excluding data with four or more missing records, and data were processed into daily averages with five or more measurement data.

According to the observational data shown in Fig.1, the average wind speed was confirmed to be 5.34 m/s, with the most severe wind recorded at a daily average of 14.1 m/s. The highest wind speed recorded were 21.8 m/s. The average atmospheric pressure is 1017.0 hPa, and the highest recorded value for atmospheric pressure is 1039.4 hPa as per time-recorded values.

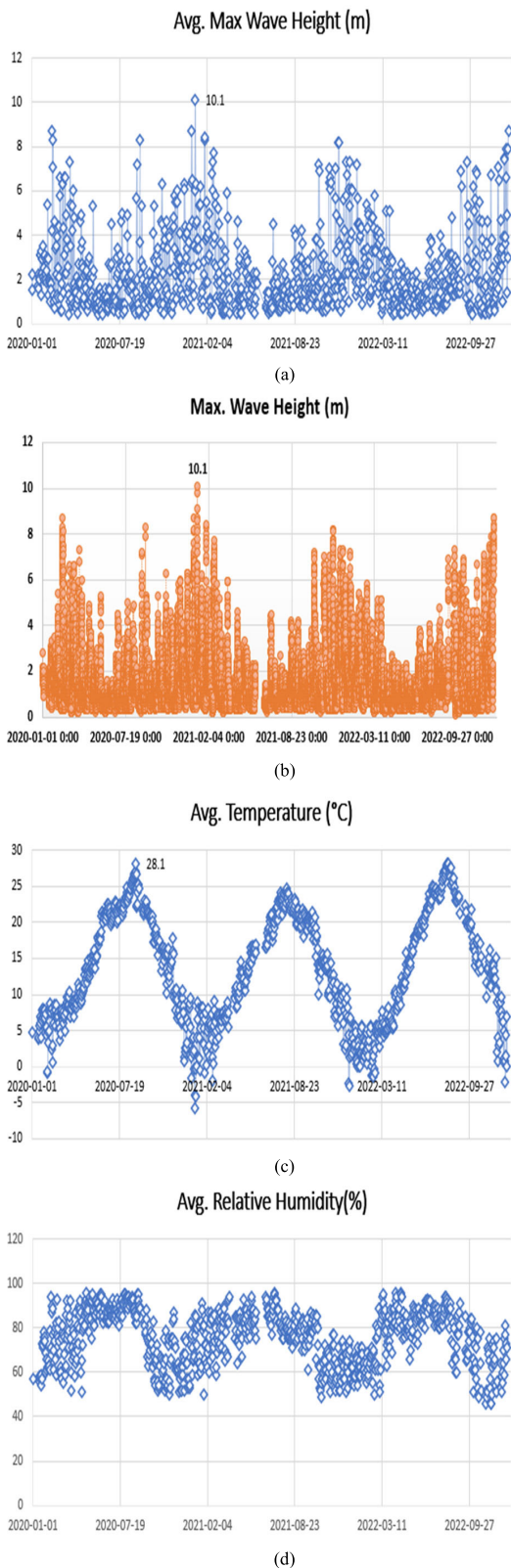


FIGURE 2. Other environmental data at Buan, Korea: (a) daily averaged maximum wave height; (b) instantaneous maximum wave height; (c) daily averaged temperature; (d) daily averaged humidity.

According to the observational data in Fig.2, the average wave height is 2.32 m, with the highest recorded value for

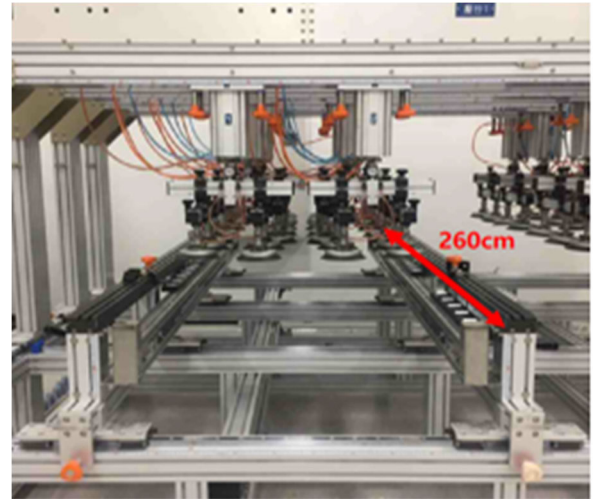


FIGURE 3. Dynamic mechanical loading tester.

wave height being 10.1 m as per time-recorded values. The average temperature is 13.4 °C, and the average humidity is confirmed to be 75%.

The natural environments are listed in Table 1. It summarizes the data for the average conditions and the worst conditions at their maximum values. The numerical values of the forces exerted on the structures were calculated by converting the naturally occurring conditions of wind, atmospheric pressure, and wave height into organized forces.

To convert the environmental data into numerical values, a consistent structural area of 1 m² is used, and the data was transformed accordingly. The values influenced by the wave height were transformed into vertical direction values using sine function. Through this process, the data of the environmental conditions was calculated, resulting in an average force of 5,854 and a maximum force of 25,671.

Through the analysis of data confirmed by offshore observations, factors suitable for simulation and practical experimentation were reviewed, allowing for predictions and analyses of the presumed environment in this paper. It was noted that there were aspects unchanged that could serve as a basis for actual simulations and experiments regarding environmental variables not considered in the experiments of this paper. While it is not expected that unconsidered environmental variables will drastically alter the overall experimental results concerning the marine environment, efforts could be made to incorporate such variables for continuous improvement in the future.

III. MECHANICAL STRESS EVALUATION

Experiments conducted on structures to evaluate the potential pressure exerted on modules in natural environments in Fig 3. The results of these structural experiments were validated through simulations. Experimental evaluations using pressure pads were conducted to apply direct stress and pressure to the PV modules [15], [16]. The experiments were conducted

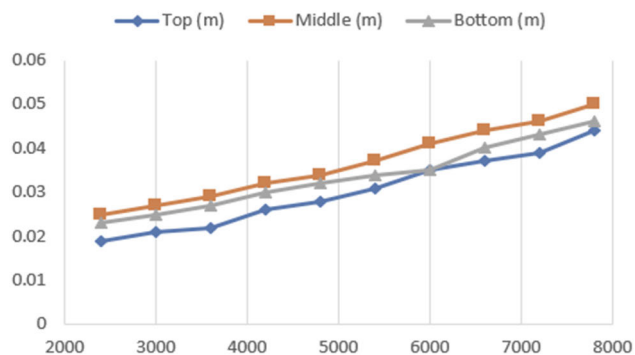


FIGURE 4. Deformation of dynamic mechanical loading test.

using a dynamic mechanical load tester as shown in Fig. 3, utilizing KING DESIGN's KDMI01 product [17]. The dynamic mechanical load tester is designed to regulate air pressure and test the mechanical load of PV module. The external dimensions of the equipment are L 360 × D 260 × H 185 cm. Loads are transmitted to the vacuum suction cups through crossbars and columns. Each vacuum suction cup is equipped with a vacuum level indicator, and each cylinder can exert a pulling force of up to 45 kg between the suction cup and the glass. The structure consists of a piston with a diameter of 150mm and a depth of 120mm, each attached with 4 suction cups. They are arranged in a 4 × 4 array on both sides. Direct pressure is applied vertically for dynamic mechanical load testing. The distance between the suction cups is set to 100mm within the possible range of 120mm to 400mm for dynamic mechanical load testing.

The PV module supports are at the top, middle, and bottom positions of the panel. The long side is supported by three structures, and the supports are fixed at positions of 43/96/139cm. The bending degree in the horizontal direction relative to the vertical upward direction was measured, including parameters such as the initial output of the module. The pressure values confirmed through natural data were set, and stress was applied at each step accordingly from 2400Pa to 7800Pa. The load stress was applied to the PV module by applying over an hour with each pressure pad considering the entire area of the PV module. Parameters were measured using a PV simulator (PASAN). The degree of bending at the top, middle, and bottom positions was measured at this time. An EL test was conducted on the PV module to confirm the normality of the PV cells after collecting the measured data.

The deformation of the PV module, confirmed through the pressurization experiments, was assessed by measuring the extent of deformation after each experiment, as shown in Fig.4. This enabled a comparison with the results of existing simulations. As the pressure increased, deflection occurred around the center of the module. The module was securely fixed using sturdy support structures at the top, middle, and bottom. Increasing the pressure on the suction pads leads to bending and deflection.

The deformation due to pressure on the PV module is a crucial aspect. PV module was first placed on the dynamic

mechanical load test equipment to conduct experiment, and the initial values were then verified. As described in the experimental process, the supports for the PV module are positioned at 43/96/139cm. The deflection in the horizontal direction relative to the vertical uplift from the supports of the PV module is measured. To conduct mechanical load testing, the pressure was then applied using suction pads for over an hour, and the deflection relative to the base supports was measured after the stress applied to the PV module had dissipated. Accuracy was considered from the initial data. The module deflection, caused by its own weight, was excluded from the initial data review based on trend analysis.

Through the experiments, it is possible to confirm the strength and durability of the PV module. The deformation from dynamic mechanical loading and each electrical characteristic is confirmed. The deformation of PV modules enables the prediction of structural changes occurring in natural environment. The electrical characteristics enable the anticipation of output values of PV modules according to the influence based on experimental results. PV modules are installed across diverse regions, including FPV modules on aquatic bodies. FPV modules exposes to a wider range of natural conditions than ground-mounted PV influencing both output variations and module selection.

Based on the study result, it is possible to access the expected durability and output of PV modules and select PV modules suitable for installation at ocean environments. Interpretation of the electrical values confirmed through pressurization experiments can be performed using the results of each parameter in Fig.5. The characteristics of the module based on the pressure can be identified. As the pressure increased, the rates of decrease of the short circuit current (ISC) and open circuit voltage (VOC) were barely noticeable. The output of the module dropped by up to 93% from the initial voltage at 3600 Pa, with a 14% reduction in the output compared to the previous one at 4800 Pa. At 7,800 Pa, an output reduction of 67% was observed. The ISC and VOC were not significantly affected by the applied pressure, but the fill factor and output of the PV module significantly decreased, exceeding 33% at 7,800 Pa. This was attributed to the increase in the serial resistance (RS) owing to the impact on the PV cells inside the module caused by cracks and damage, resulting in a decrease.

To analyze experiment, the EL test results measured after the pressurization experiment were interpreted, as shown in Fig.6. As the pressurization test progressed, cracks in the PV cells inside the module, were confirmed through an EL test. Starting from 6000 Pa in the pressurization, there was a rapid increase in cracks in the PV cell, resulting in a subsequent decrease in the output. Cracks originating from the external pressure on the cell gradually increase, emerging as a major cause of output degradation.

IV. STRESS SIMULATION

A simulation was conducted to assess the impact of forces on the PV module under natural environmental conditions.

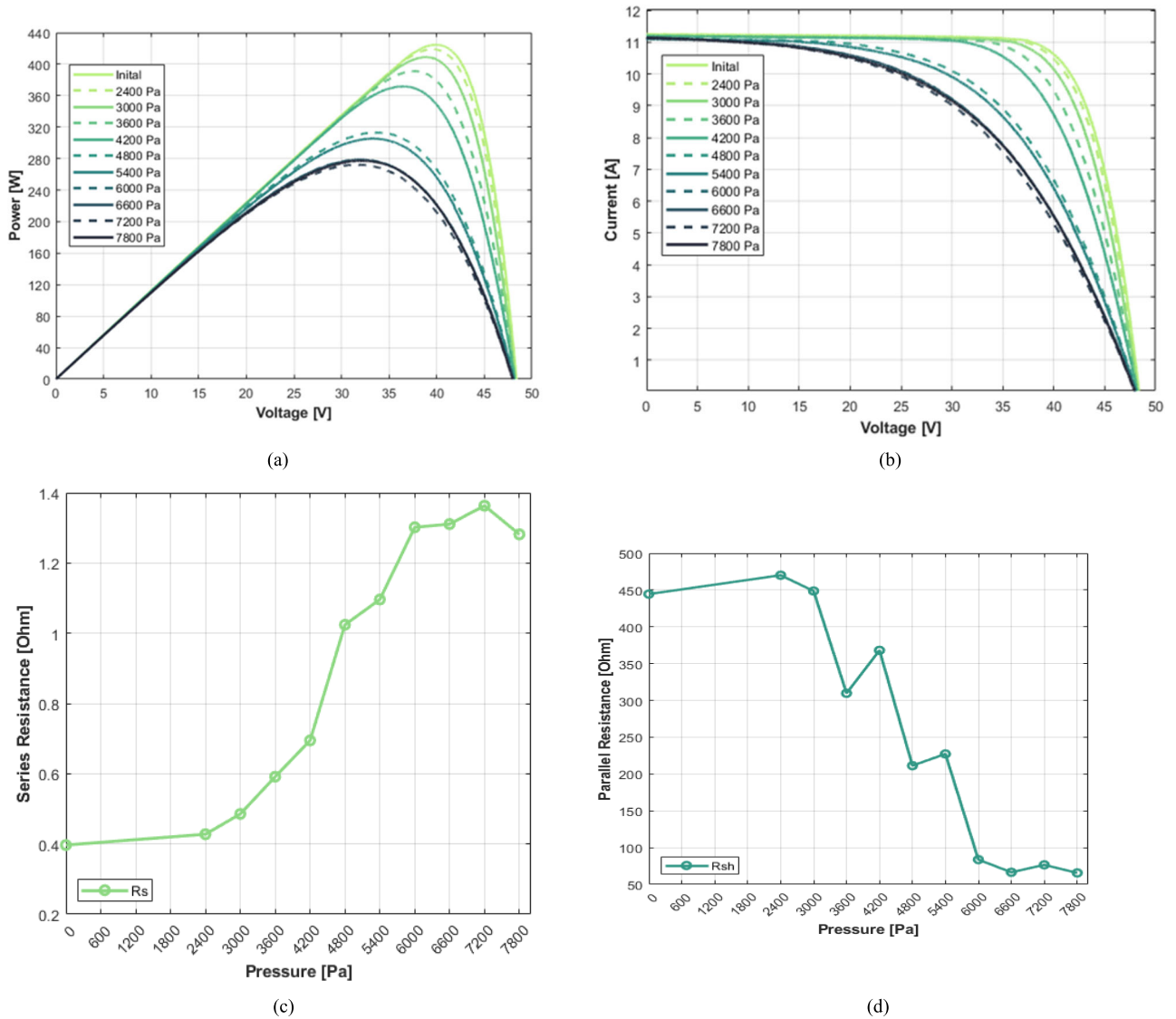


FIGURE 5. Data of dynamic mechanic loading tests: (a) I-V curves; (b) P-V curves; (c) series resistances; (d) parallel resistances.

Environmental data values applied, and simulations were performed at module level including the cells in PV module. All of material characteristics used in the structure of the PV module, including glass, EVA, cells, and back-sheets, were verified to conduct the simulation. The PV module used in the simulation was the SINSUNG E&G SS-DM420DG with an output of 433 W. The detailed product information is provided in Fig.7 for the module structure and in Table 2 for the physical parameters.

Simulation results based on material characteristics confirmed through dynamic force showed a real measurement deviation within 5% compared to the simulation results, demonstrating sufficient validity. Based on these results, the simulation can serve as a substitute for the experimental outcomes, facilitating simulations of worst-case weather scenarios.

TABLE 2. Specification of sinsung E&G module.

SS-DM420DG	Data	Unit
Module Size	1,939 x 1,116 x 35	mm
Module Efficiency	19.41	%
Cell Area	156.75 x 156.75	mm
Module Weight	24.2	Kg
PV cell output	5.16	W
Pmax	433.76	W
Voc	48.22	V
Isc	11.38	A
Vmax	40.38	V
Imax	10.74	A

To conduct simulations of the PV module, the structure and characteristics of each material used in the PV module were analyzed. The material characteristics obtained from

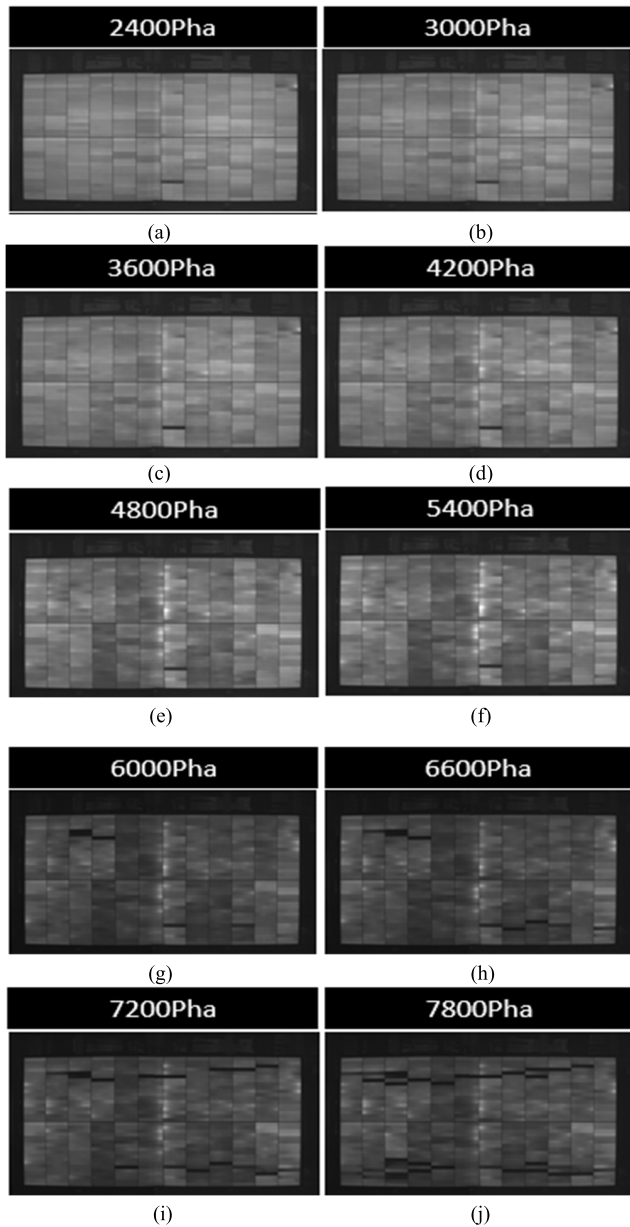


FIGURE 6. EL images of the dynamic mechanical loading test; (a) 2400Pa; (b) 3000Pa; (c) 3600Pa; (d) 4200Pa; (e) 4800Pa; (f) 5400Pa; (g) 6000Pa; (h) 6600Pa; (i) 7200Pa; (j) 7800Pa.

TABLE 3. Material property of sinsung E&G module.

Material	Density [g/cm ³]	Young's Module [Pa]	Poisson's Ratio	Tensile Strength [Pa]
Glass	2.5	6.7 x 1,010	0.23	1.2 x 10 ⁸
EVA	0.875	2.0 x 10 ⁷	0.50	3.0 x 10 ⁸
Cells	2.329	1.25 x 1,011	0.28	1.7 x 10 ⁸
Backsheet	1.4	3.0 x 10 ⁹	0.35	1.2 x 10 ⁸
Rubber	1.45	1.5 x 10 ⁶	0.50	3.0 x 10 ⁶
Frame	2.69	6.9 x 1,010	0.33	1.87 x 10 ⁸

this analysis, are summarized in the Table 3. The module used in the simulation was composed of shingled string cells and

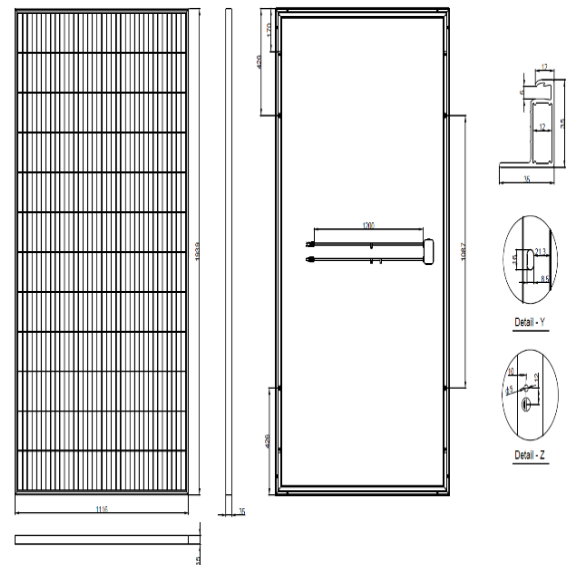


FIGURE 7. Module structure image.

PERC technology, with the space between the EVA and cells filled with EVA. The post curing density of EVA is between 4.8 and 5.0 g/cm³, and the adhesive strength is 20 kgf. Each material property was based on the data provided by the manufacturer and simulations were conducted by verifying the material properties for each manufacturer's model.

The simulation for the PV module utilized models and characteristics provided by the manufacturer. However, variations and factors that could occur during the manufacturing process of PV modules or during installation were excluded from the simulation. To create an environment as close as possible to the evaluation results of the experiments, the simulation incorporated the PV frame structure, including the string cell 432 used in the simulation. After analyzing the compressive load for a single PV module, simulations including the structure of the FPV 6 x 4 system were conducted. All simulations assumed that the properties provided by the manufacturer are accurate, and the error range for simulations was defined as +/- 5%.

A primary stress simulation of a single PV module was conducted to assess the degree of deformation based on the force applied to the module. Interpretation was performed using the values obtained from the natural data on the pressure applied to the PV module, considering the average values and deviations below and above the mean.

The material properties of the module were considered in the simulation. In the simulation, when pressure was applied to the PV module, a direct and noticeable change in the shape of the deflection occurred, particularly at the central module, as shown in Fig.8 and Fig.9. The PV module framed along its edges, experiences the most stress, primarily originating from the center of the module. This is confirmed through simulations.

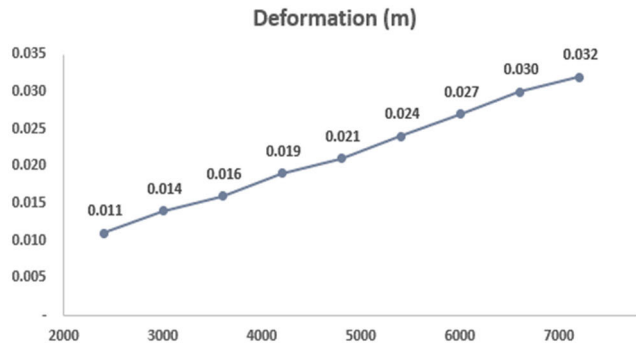


FIGURE 8. Simulation result of PV module deformation.

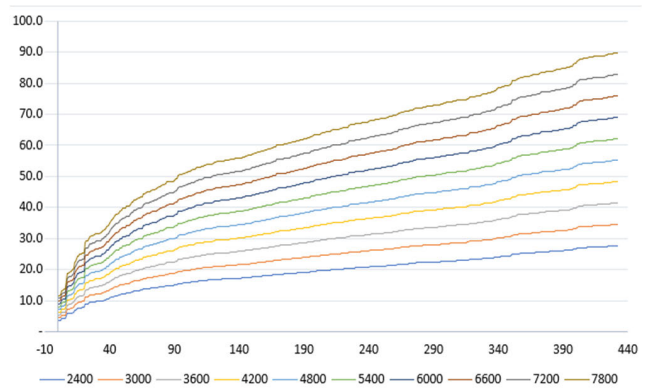


FIGURE 11. Simulation result of deformation of each cell.

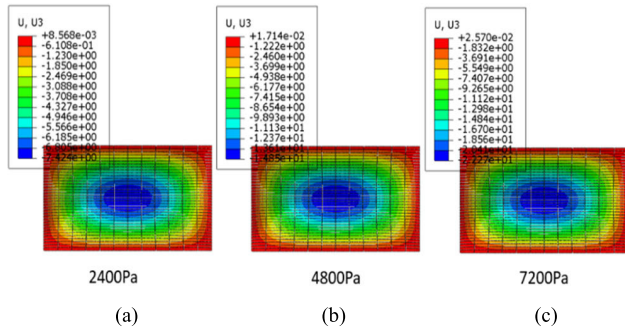


FIGURE 9. Shapes of deflection: (a) 2400Pa; (b) 4800Pa; (c) 7200Pa.

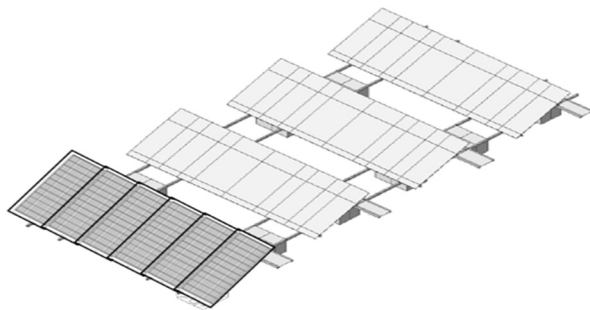


FIGURE 10. Floating PV generation system (6 × 4).

To simulate a PV power plant installed on water, an analysis of the basic module, including the frame structure shown in Fig.10, was conducted. The simulation of the water-based PV power plant was configured with a 4-row structure, vertically arranging six PV modules, and individual simulations were conducted for each frame structure [18].

The frame structure of the floating PV system for the simulation used an actual FPV power generation system. The structure has a width of 6.4 meters and a length of 6.7 meters alloy-coated steel, with 12 count PV modules installed per unit. It is designed in the form of two combined unit structures. The design and seismic design of the structure were reviewed based on the Shore Protection Manual (1984, USACE, Coastal Engineering Research) and BS 6349,

1-7 (2000, Euro Code), and simulations and verification of the structure were conducted.

The simulations examined the varying degrees of deformation induced by the forces applied to each module and cell. In the simulation, 432 string cells were used and the deformation of each cell caused by the applied forces was analyzed. From the simulation results, based on the extent of deformation of each cell, predictions regarding the structural changes in the cells according to environmental conditions can be made, as shown in Fig.11.

The simulation results for the PV power plant installed on water, as showed in Fig.12, indicate that, consistent with previous experiments, an increase in pressure led to deformation at both the module and individual cell levels. An analysis of the results, including various structures, also indicated that the deformation of each cell increased with applied pressure.

The composition of materials of PV modules are crucial factors in both the experiments and simulations of this study. Material properties utilized in simulations were therefore significantly reflected to describe the composition and structure of PVs and to analyze deformations. This study anticipated preliminary outputs through experiments and simulations analyzing natural environments including marine ones. The characteristics of materials comprising PV modules and FPV systems can have various impacts on experiments and simulations of structures. Especially, the diverse properties of materials constituting PV modules can influence their durability and long-term reliability against external forces. It is deemed possible to conduct various research on PV modules with characteristics tailored to ground-mounted PV and marine PV generation by making changes to the structure and materials of the various cells constituting PV. It is however crucial to maintain a balance in combinations with considerations of coefficients of thermal expansion (CTE) between materials to alter material properties and characteristics.

V. DATA ANALYSIS

Based on the electrical characteristic data confirmed through pressurization experiments, an estimation was conducted at the point where the module underwent degradation. This

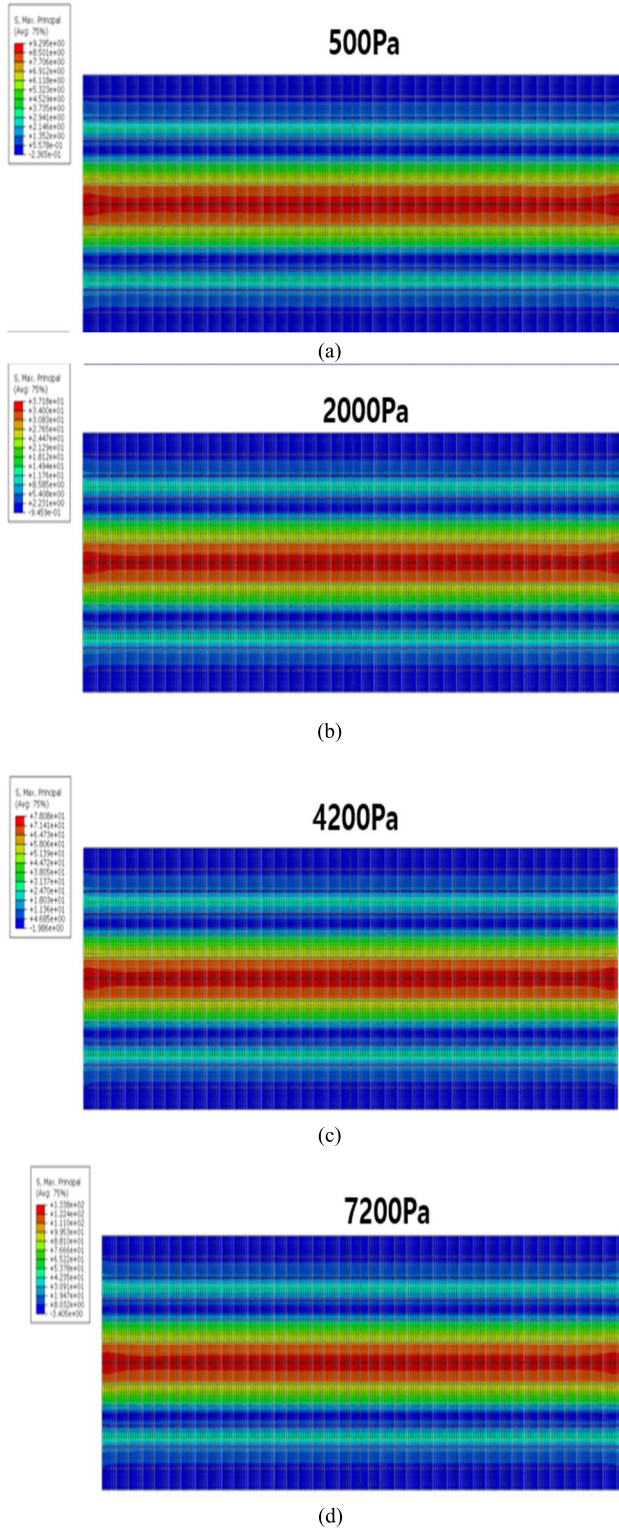


FIGURE 12. Simulation result of PV generation system (6 × 4): (a) 500Pa; (b) 2000Pa; (c) 4200Pa; (d) 7200Pa.

process can then be performed to enable advanced prediction and modeling of natural environmental factors. Each set of electrical experimental data was organized into graphs to

review the degradation model using linear regression. The correlation of the output through linear regression, focusing on the mechanical experiments, were analyzed.

The reliability of PV modules and the power generation capacity of PV systems continuously decrease over time. Understanding the degradation process of PV modules allows one to anticipate their maximum utilization during their expected lifespan. The PV degradation occurs due to various environmental factors. Degraded PV modules exhibit abnormalities in output due to various defects such as cell cracks, delamination, hot spots, glass soiling, EVA browning, and coating oxidation, among others. PV modules are then subject to various degradation models and patterns due to climatic and environmental factors as they are exposed to diverse external conditions. The FPV modules exposed to marine environmental climates require research into degradation different from that of ground PV modules. The results of this study enable to anticipate the resilience of PV to degradation over time and environmental conditions, as well as the expected replacement time for the modules.

The degradation model was tested by referencing the values from PV modules installed in the field for over 11 years [19]. The power loss of PV systems generally tends to increase over time, with the mismatch in output of PV modules becoming more pronounced. The degradation model used in this study is based on simulation research of the degradation process of modules installed in the field for 11 years. Using data collected from the field, the PV characteristics based on environmental conditions and PV module aging factors were described using a circuit-based model. The analysis of PV degradation factors revealed that the main cause of power loss is the decrease in short circuit current. Factors contributing to degradation in PV modules installed in the field initially were identified, and a model was proposed through regression modeling. The fundamental assumption for the data analysis did not consider the time elapsed in the mechanical experiments, but rather assumed changes from the initial measurements. From the results of the mechanical experiments shown in Fig. 13, R_s continuously increased, reaching 350% of the initial value, whereas the parallel resistance (R_{sh}) decreased to approximately 10% of the initial value. It is also notable that all degradation factors for the marine environment could be substituted to pressure. Based on linear regression and results of Fig. 13, P_s and P_{sh} modeling represented as (7) and (8). The pressure causes degradations of series and parallel resistance as shown in Fig. 13. From these results, a degradation model of output over time was obtained [20].

The field aged module degradation modeling represented by (1), (2). $R_{d,s,t}$ denotes a natural degradation of a series resistance at specific time; t denotes a specific time based yearly. $R_{s,0}$ denotes an initial series resistance. As denotes a natural degradation rate of a series resistance. $R_{d,sh,t}$ denotes a natural degradation of a parallel resistance. $R_{sh,0}$ denotes an initial parallel resistance. A_{sh} denotes a natural degradation rate of a parallel resistance. It takes the values of the field aged

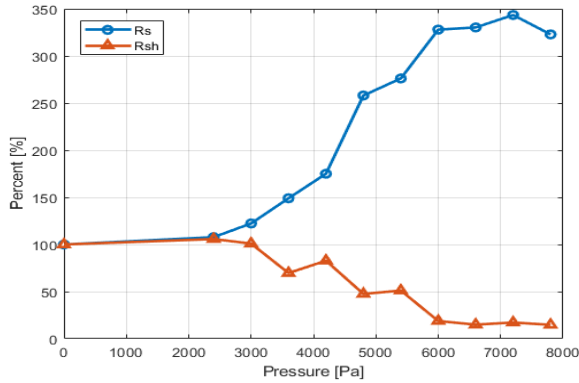


FIGURE 13. Resistance of dynamic mechanical loading test (Rs & Rsh).

module degradation modeling from [19], which is conducted in the outdoor environment.

$$R_{d,s,t} = R_{s,0} \cdot (1 + A_s \cdot t) \quad (1)$$

$$R_{d,sh,t} = R_{sh,0} \cdot (1 + A_{sh} \cdot t) \quad (2)$$

The forced degradation modeling applying the analysis of marine environmental condition represented by (3), (4). $R_{f,s,t}$ denotes a forced degradation of a series resistance caused by the marine environmental conditions. $R_{f,sh,t}$ denotes a forced degradation of a parallel resistance caused by the marine environmental conditions. P_s denotes a degradation rate of a series resistance caused by the marine environmental conditions. P_{sh} denotes a degradation rate of a parallel resistance caused by the natural environmental conditions. Each degradation rate is based on the results of Fig.13, and 1 is subtracted to consider only additional degradation effects caused by the marine environment.

$$R_{f,s,t} = R_{s,t-1} \cdot (P_s - 1) \quad (3)$$

$$R_{f,sh,t} = R_{sh,t-1} \cdot (P_{sh} - 1) \quad (4)$$

The final degradation suggested is obtained by combining the result of the field aged model and result of the forced model caused by the marine environment. The modeling calculations showed that (5) and (6). $R_{s,t}$ denotes a total degradation of a series resistance. $R_{sh,t}$ denotes a total degradation of a parallel resistance.

$$R_{s,t} = R_{d,s,t} + R_{f,s,t} \quad (5)$$

$$R_{sh,t} = R_{d,sh,t} + R_{f,sh,t} \quad (6)$$

Based on linear regression and results of Fig.13, P_s and P_{sh} are then represented as (7) and (8) respectively. Coefficients of the linear regression are expressed separately; a_4 to a_0 are the coefficients of P_s and b_4 to b_0 are the coefficients of P_{sh} . P_a denotes an equivalent pressure of the natural environmental conditions.

$$P_s = a_4 \cdot P_a^4 + a_3 \cdot P_a^3 + a_2 \cdot P_a^2 + a_1 \cdot P_a + a_0 \quad (7)$$

$$P_{sh} = b_4 \cdot P_a^4 + b_3 \cdot P_a^3 + b_2 \cdot P_a^2 + b_1 \cdot P_a + b_0 \quad (8)$$

From the results shown in Fig.14, the resistance values first vary in the overall ranges. Using linear regression modeling,

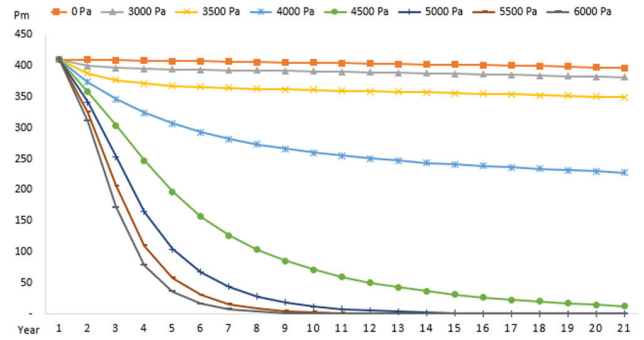


FIGURE 14. Data analysis and modeling result.

the variation in R_s and R_{sh} can be expected, in addition to anticipating the output values. Output degrades over time owing to external forces, leading significant degradation, observed particularly after three years. Notably, the modules subjected to an external force of 4500 Pa exhibited a drastic decline in the output power.

VI. CONCLUSION

In this study, the research on the natural data of PV modules has been conducted to investigate the impact of the natural environment on actual PV modules and PV power generation. Simulations were conducted on offshore FPV modules and PV power plants to verify the effects of the natural environment. Structural experiments were conducted to observe deformations owing to pressure and changes in the output, including electrical parameters, in the natural environment. Structural experiments predicted that the mechanical strength of PV modules could be confirmed through deformation and impact assessments in a natural environment.

1) The natural environment varies regionally, affecting various factors, such as wind speed, atmospheric pressure, humidity, and temperature, which in turn impact external structures, including PV modules. The influences of wind and waves identified in this study are crucial factors in offshore PV research, emphasizing the need for prior geographic analysis.

2) An analysis of the impacts on the natural environment was conducted using climatic data based on geographical locations, directly applied to simulate PV modules. The simulation results enable the prediction of PV power facilities, including PV modules, under specific environmental conditions.

3) Structural experiments assessed the environmental factors, revealing module deformations of up to 0.05 m. As a result, the fill factor and output of the PV modules significantly decreased by more than 33% at 7,800 Pa, which was attributed to internal cracks and damage caused by the applied load on the PV modules.

4) The output from the structural experiments decreased by 93% at 3600 Pa and by a further 14% reduction at 4800 Pa compared to the initial voltage, indicating the need for maintenance and replacement of the modules. This highlights the

importance of pre-evaluating the reliability and failure of modules based on actual environmental data.

5) In this study, all the data on environmental conditions were obtained and used for prediction of outputs in natural settings. It is expected that considering the geographical climate in the generation of PV modules will allow for optimal site selection for PV power plants.

6) The simulation results and structural experimental data from this study can serve as predictive information for module deformation. Utilizing the predictable results, future research can enhance the material characteristics and design structures more suitably for the natural environment in the construction of offshore PV power plants. Also, the simulation results denote that how much more PV power plant is deteriorated by marine factors than the land. These results must be reflected and considered in an economic evaluation of floating and marine PV systems because of their accelerated degradations.

This paper conducted simulations and experimental evaluations based on data confirmed through ocean environments. It is anticipated that through various reviews of PV based on property analyses for simulations considering diverse geographical characteristics, an optimized FPV can be proposed. Continuous research will be conducted to propose the optimal FPV in advance by optimizing factors that may arise in the manufacturing process, including reliability of FPV system.

7) There are multiple marine environmental data which can be obtained through multiple observation stations. For example, the Meteorological Administration in Korea collects data from 26 meteorological observation stations and provides related ocean environment data. This data could then be used in further studies, including research on climate change. The analysis of the coastal area used in this study may lead to further research based on data collected before and after the construction of PV power plants. In maritime areas, various climatic environments such as typhoons, waves, and winds occur along with geographical characteristics. To develop maritime areas, PV modules suitable for generation based on simulations and output estimation for FPV can be selected. Location selection can be also carried out considering the climate environment based on the selection and reliability of PV modules. As confirmed in this study, FPV could be considered in relatively mild maritime environments. Locations where the sea extends deeply inland beyond the coastline, such as reclaimed land, gulfs, and bay areas, can be proposed as optimal locations for FPV. Further research would be needed to analyze the environmental conditions for the regions specified based on this analysis.

8) In this study, cost was not considered, indicating the need for future research in this area. It would however range now from 1.2 to 1.5 M\$/MW after pre and mass production evaluation. Specifically, in terms of sustainability and energy efficiency, it is necessary to anticipate the suitability of geographical locations in advance, considering factors such as wave and wind size in maintenance and operation aspects. It is therefore expected that systems with maximum

efficiency in terms of maintenance and operation can be obtained.

ACKNOWLEDGMENT

The authors would like to appreciate SCOTRA Company Ltd., for providing valuable data.

REFERENCES

- [1] Z. Liu, S. E. Sofia, H. S. Laine, M. Woodhouse, S. Wiegbold, I. Marius Peters, and T. Buonassisi, "Revisiting thin silicon for photovoltaics: A technoeconomic perspective," *Energy Environ. Sci.*, vol. 13, pp. 12–23, May 2020, doi: [10.1039/D0TA04575F](https://doi.org/10.1039/D0TA04575F).
- [2] *Renewables 2023*, IEA, Paris, 2024. [Online]. Available: <https://www.iea.org/reports/renewables-2023>
- [3] S. Ong, "Land-use requirements for solar power plants in the United States," Nat. Renew. Energy Lab. (NREL), Golden, CO, USA, Tech. Rep. NREL/TP-6A20-56290, 2013.
- [4] M. Bolinger and G. Bolinger, "Land requirements for utility-scale PV: An empirical update on power and energy density," *IEEE J. Photovolt.*, vol. 12, no. 2, pp. 589–594, Mar. 2022, doi: [10.1109/JPHOTOV.2021.3136805](https://doi.org/10.1109/JPHOTOV.2021.3136805). <https://doi.org/10.1109/JPHOTOV.2021.3136805>.
- [5] R. Cazzaniga and M. Rosa-Clot, "The booming of floating PV," *Sol. Energy*, vol. 219, pp. 3–10, May 2021, doi: [10.1016/j.solener.2020.09.057](https://doi.org/10.1016/j.solener.2020.09.057).
- [6] T. Kjeldstad, D. Lindholm, E. Marstein, and J. Selj, "Cooling of floating photovoltaics and the importance of water temperature," *Sol. Energy*, vol. 218, pp. 544–551, Apr. 2021, doi: [10.1016/j.solener.2021.03.022](https://doi.org/10.1016/j.solener.2021.03.022).
- [7] S. Gadzanku, "Enabling floating solar (FPV) deployment: Policy and operational considerations," Nat. Renew. Energy Lab. (NREL) Asia Clean Energy Forum, Golden, CO, USA, Tech. Rep. NREL/PR-7A40-83228, Jun. 2022.
- [8] E. L. Meyer and E. E. van Dyk, "Assessing the reliability and degradation of photovoltaic module performance parameters," *IEEE Trans. Rel.*, vol. 53, no. 1, pp. 83–92, Mar. 2004, doi: [10.1109/tr.2004.824831](https://doi.org/10.1109/tr.2004.824831).
- [9] Y. Zhou, M. Yuan, J. Zhang, G. Ding, and S. Qin, "Review of vision-based defect detection research and its perspectives for printed circuit board," *J. Manuf. Syst.*, vol. 70, pp. 557–578, Oct. 2023, doi: [10.1016/j.jmsy.2023.08.019](https://doi.org/10.1016/j.jmsy.2023.08.019).
- [10] P. Ranjbaran, "A review on floating photovoltaic (FPV) power generation units," *Renew. Sustain. Energy Rev.*, vol. 110, pp. 332–347, Jul. 2019, doi: [10.1016/j.rser.2019.05.015](https://doi.org/10.1016/j.rser.2019.05.015).
- [11] W. Shi, C. Yan, Z. Ren, Z. Yuan, Y. Liu, S. Zheng, X. Li, and X. Han, "Review on the development of marine floating photovoltaic systems," *Ocean Eng.*, vol. 286, no. 1, 2023, Art. no. 115560, doi: [10.1016/j.oceaneng.2023.115560](https://doi.org/10.1016/j.oceaneng.2023.115560).
- [12] M. Maurizi, C. Gao, and F. Berto, "Predicting stress, strain and deformation fields in materials and structures with graph neural networks," *Sci. Rep.*, vol. 12, no. 1, Dec. 2022, doi: [10.1038/s41598-022-26424-3](https://doi.org/10.1038/s41598-022-26424-3).
- [13] M. Aghaei, A. Fairbrother, A. Gok, S. Ahmad, S. Kazim, K. Lobato, G. Oreski, A. Reinders, J. Schmitz, M. Theelen, P. Yilmaz, and J. Kettle, "Review of degradation and failure phenomena in photovoltaic modules," *Renew. Sustain. Energy Rev.*, vol. 159, May 2022, Art. no. 112160, doi: [10.1016/j.rser.2022.112160](https://doi.org/10.1016/j.rser.2022.112160).
- [14] Open MET Data Portal. *KMA Weather Data Service*. [Online]. Available: <https://kma.go.kr>
- [15] S. Kajari-Schröder, I. Kunze, U. Eitner, and M. Köntges, "Spatial and orientational distribution of cracks in crystalline photovoltaic modules generated by mechanical load tests," *Sol. Energy Mater. Sol. Cells*, vol. 95, no. 11, pp. 3054–3059, Nov. 2011, doi: [10.1016/j.solmat.2011.06.032](https://doi.org/10.1016/j.solmat.2011.06.032).
- [16] M. Köntges, I. Kunze, S. Kajari-Schröder, X. Breitenmoser, and B. Bjørneklett, "The risk of power loss in crystalline silicon based photovoltaic modules due to micro-cracks," *Sol. Energy Mater. Sol. Cells*, vol. 95, no. 4, pp. 1131–1137, Apr. 2011, doi: [10.1016/j.solmat.2010.10.034](https://doi.org/10.1016/j.solmat.2010.10.034).
- [17] K. Desing. *Dynamic Mechanic Loading Tester*. [Online]. Available: <https://www.kdi.tw/en/product-256753/Dynamic-Mechanic-Loading-Tester.html>
- [18] A. Ghosh, "A comprehensive review of water based PV: Flotovoltaics, under water, offshore & canal top," *Ocean Eng.*, vol. 281, Aug. 2023, Art. no. 115044, doi: [10.1016/j.oceaneng.2023.115044](https://doi.org/10.1016/j.oceaneng.2023.115044).

- [19] C. Huang and L. Wang, "Simulation study on the degradation process of photovoltaic modules," *Energy Convers. Manag.*, vol. 165, Jul. 2018, pp. 236–243, doi: [10.1016/j.enconman.2018.03.056](https://doi.org/10.1016/j.enconman.2018.03.056).
- [20] G. G. Kim, J. H. Choi, S. Y. Park, B. G. Bhang, W. J. Nam, H. L. Cha, N. Park, and H.-K. Ahn, "Prediction model for PV performance with correlation analysis of environmental variables," *IEEE J. Photovolt.*, vol. 9, no. 3, pp. 832–841, May 2019, doi: [10.1109/JPHOTOV.2019.2898521](https://doi.org/10.1109/JPHOTOV.2019.2898521). <https://doi.org/10.1109/JPHOTOV.2019.2898521>



BYEONG YONG LIM received the B.S. degree in electrical and electronic engineering from Hongik University and the M.S. degree from the Next Generation Photovoltaic Module and Power System Research Center, Konkuk University, Seoul, South Korea, in 2020, where he is currently pursuing the Ph.D. degree. His research interests include the reliability of solar cells, PV modules, and fault detection of power generation systems of floating PVs for RE100.



SEONG-HYEON AHN received the B.S. degree from Konkuk University, Seoul, South Korea, in 2023, where he is currently pursuing the M.S. degree in electrical engineering with the Next Generation Photovoltaic Module and Power System Research Center. His research interests include PV power system diagnosis with power index and the fusion of renewable energy resources for RE100.



MIN SOO PARK received the B.S. and M.S. degrees in mechanical engineering from Yeungnam University, South Korea, in 2002, and the Ph.D. degree in mechanical engineering from Texas A&M University, College Station, TX, USA, in 2009. Before the Ph.D. degree, he was with the Department of Engineering Science and Applied Mathematics, Northwestern University, IL, USA, from 2004 to 2006. His research interests include the optimization of conventional PKG and

WLPKG by using computational methods.



JIN HO CHOI received the B.S., M.S., and Ph.D. degrees in electrical engineering from Konkuk University, Seoul, South Korea, in 2018, 2019, and 2023, respectively. He is currently with Chungbuk Techno Park (CBTP), Chungbuk, South Korea. His research interests include power prediction and fault detection of floating and marine photovoltaics using high-density PV modules (HDM) for RE100.



HOONJOO CHOI received the B.S. degree in environmental engineering from Yonsei University, South Korea, in 2004, and the M.S. degree from the Next Generation Photovoltaic Module and Power System Research Center, Konkuk University, Seoul, South Korea, in 2015, where he is currently pursuing the Ph.D. degree. His research interests include digital operation and maintenance for photovoltaic power generation system improvement and health management under a variety of environments.



HYUNG-KEUN AHN (Member, IEEE) received the B.S. and M.S. degrees in MOSFETs in electrical engineering from Yonsei University, Seoul, South Korea, in 1983 and 1985, respectively, and the Ph.D. degree in HEMTs from the Department of Electrical Engineering, University of Pittsburgh, Pittsburgh, PA, USA, in 1993. From 1986 to 1995, he was with LG Semiconductor Company, working on silicon-based device design and process integration. In 1995, he joined the Department of Electrical Engineering, Konkuk University, Seoul, where he is currently a Professor and the Dean of the Next Generation Photovoltaic Module and Power System Research and Development Center. He was the first National Photovoltaic Research and Development Program Director of the Ministry of Knowledge Economy, South Korea, from 2009 to 2011. From 2014 to 2016, he was a Foreign Professor with the Department of Electrical and Control Engineering, Division of Electrical Engineering, Shandong University of Technology (SDUT), Zibo, Shandong, China. He is also working on the design of a microgrid network for net-zero energy houses and towns using EMS, ESS, and bifacial and shingled PV modules, applicable to floating and marine PVs under the demand response control for RE100. His research interests include the reliability of both Si and GaAs-based solar cells and PV modules for applications in micro roof-top to largescale PVs connected with ESS, focusing on failure analysis, reliability, and maintenance, repair, and operation (MRO). He was a Committee Member of the National Science and Technology Commission, Energy Department, South Korea, from 2005 to 2007.

...